

Article

Thorium(IV) and Uranium(IV) Phosphaazaallenes

 Pokpong Rungthanaphatsophon, O. Jonathan Fajen, Steven P. Kelley and Justin R. Walensky * 

Department of Chemistry, University of Missouri, Columbia, MO 65211, USA

* Correspondence: walenskyj@missouri.edu; Tel.: +1-573-882-0608

Received: 10 July 2019; Accepted: 17 August 2019; Published: 21 August 2019



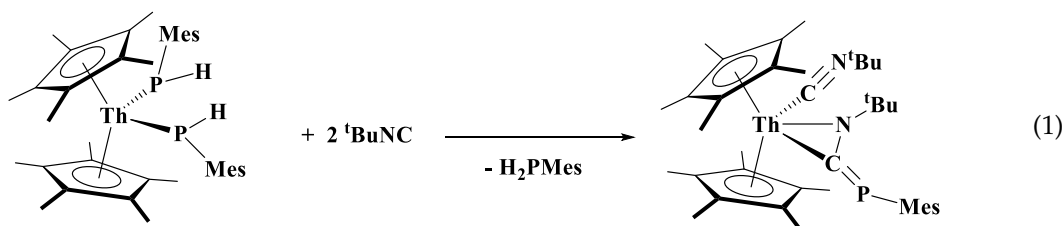
Abstract: The synthesis of tetravalent thorium and uranium complexes with the phosphaazaallene moiety, $[N(^t\text{Bu})C=P(\text{C}_6\text{H}_5)]^{2-}$, is described. The reaction of the bis(phosphido) complexes, $(\text{C}_5\text{Me}_5)_2\text{An}[\text{P}(\text{C}_6\text{H}_5)(\text{SiMe}_3)]_2$, An = Th, U, with two equivalents of $^t\text{BuNC}$ produces $(\text{C}_5\text{Me}_5)_2\text{An}(\text{CN}^t\text{Bu})[\eta^2-(\text{N},\text{C})-\text{N}(^t\text{Bu})\text{C}=\text{P}(\text{C}_6\text{H}_5)]$ with concomitant formation of $\text{P}(\text{SiMe}_3)_2(\text{C}_6\text{H}_5)$ via silyl migration. These complexes are characterized by NMR and IR spectroscopy, as well as structurally determined using X-ray crystallography.

Keywords: actinide; phosphido; phosphaazaallene; synthesis

1. Introduction

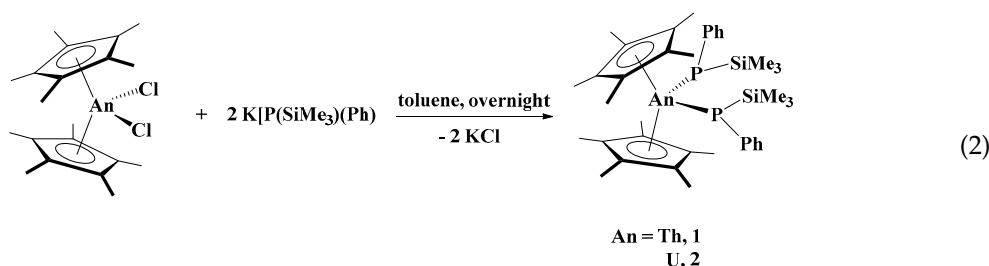
The reactivity of metal–phosphido complexes is of interest for the development of hydrophosphination catalysts as well as the synthesis of phosphorus–element multiple bonds. For example, phosphaalkenes, $\text{P}=\text{C}$, have attracted interest for building blocks in organophosphorus chemistry [1–3], ligands to transition metal complexes [4,5], as well as potential applications as functional materials [6–10]. After nearly 20 years of dormancy [11–15], actinide–phosphorus has received greater attention recently [16–19] with researchers examining similarities and differences in the molecular and electronic structure of its more studied congener, nitrogen. Our interest in actinide–phosphido complexes has been on investigating small molecule reactivity. Since actinides are large, highly electropositive metals, consequently they have an affinity to coordinate to highly electronegative atoms such as oxygen and nitrogen. Thus, they are less inclined to form strong interactions with ligands bearing soft-donor atoms such as phosphorus. Therefore, the actinide–phosphido bond should, and has been demonstrated, be relatively reactive [20–30].

Previously, we investigated the reactivity of the primary bis(phosphido) complexes, $(\text{C}_5\text{Me}_5)_2\text{Th}[\text{PH}(\text{R})]_2$, R = 2,4,6-Me₃C₆H₂ (Mes) or 2,4,6-ⁱPr₃C₆H₂ (Tipp), with $^t\text{BuNC}$ [16]. This led to a proton transfer from one phosphido ligand to form the primary phosphine, and the phosphaazaallene, $(\text{C}_5\text{Me}_5)_2\text{Th}(\text{C}\equiv\text{N}^t\text{Bu})[\eta^2-\text{N}(^t\text{Bu})\text{C}=\text{PR}]$, was isolated, Equation (1). To prevent this proton transfer, the bis(phosphido) complexes, $(\text{C}_5\text{Me}_5)_2\text{An}[\text{P}(\text{C}_6\text{H}_5)(\text{SiMe}_3)]_2$, An = Th, U, were synthesized. However, herein, we show that instead of proton transfer, silyl migration occurs, resulting in similar phosphaazaallene moieties.



2. Results

The secondary phosphido complexes, $(C_5Me_5)_2An[P(SiMe_3)(C_6H_5)]_2$, An = Th, **1**; U, **2**, were synthesized from the reaction of $(C_5Me_5)_2AnCl_2$, An = Th, U, with two equivalents of $KP(SiMe_3)(C_6H_5)$, Equation (2). Complex **2** is formed in lower yields (~40%), even when three equivalents of the potassium salt are used. This is presumably due to the steric properties of the phosphido ligand with the smaller uranium(IV) ionic radii as compared to thorium(IV) as **1** has consistent yields of >80%. The major byproduct in the reaction of $(C_5Me_5)_2UCl_2$ with two equivalents of $K[P(SiMe_3)(C_6H_5)]$ is $(C_5Me_5)_2U(Cl)[P(SiMe_3)(C_6H_5)]$, **2a**. A similar result was observed with $K[P(SiMe_3)(Mes)]$ [31]. When one equivalent of $K[P(SiMe_3)(C_6H_5)]$ is reacted with $(C_5Me_5)_2UCl_2$, then **2a** can be isolated in high yield, >90%. The 1H NMR spectrum of **1** showed resonances at 2.08 and 0.56 ppm for the $(C_5Me_5)^{1-}$ and $SiMe_3$, respectively. In addition, the ^{31}P NMR spectrum of **1** showed a resonance at 72.7 ppm, shifted downfield from $(C_5Me_5)_2Th[P(SiMe_3)(Mes)]_2$ which is located at 48.5 ppm. The paramagnetic NMR spectrum of **2** showed the $(C_5Me_5)^{1-}$ resonance at 13.5 ppm, while the $SiMe_3$ group was located at -8.94 ppm. In **2a**, the $(C_5Me_5)^{1-}$ and $SiMe_3$ resonances are observed at 13.4 ppm and -13.9 ppm, respectively. For comparison, $(C_5Me_5)_2U(PPh_2)_2$ and $(C_5Me_5)_2U(CH_3)(PPh_2)$ have resonances for $(C_5Me_5)^{1-}$ located at 12.17 and 11.08 ppm, respectively [32].



The structures of **1** and **2**, Figure 1, were determined by X-ray crystallographic analysis. The metal–phosphorus bond distances are 2.8243(9) Å in **1** and 2.7477(8) and 2.7478(8) Å in **2**, while the P–M–P bond angles are 92.75(5) and 92.16(4)° in **1** and **2**, respectively. In **1**, the thorium–phosphido bond distances are similar to other metallocene thorium bis(phosphido) complexes reported and slightly shorter than the 2.855(6) and 2.938(6) Å in $Th(Bc^{Mes})_2[PH(Mes)]_2$ [33]. Complex **2** is the first structurally characterized bis(phosphido) uranium complex, however polyphosphide complexes of uranium are known from P_4 activation [34,35]. The uranium–phosphido bond distances are shorter than those in $U(Tren^{TIPS})(PH_2)$ of 2.883(2) Å [36], but similar to the 2.789(4) Å in $(C_5Me_5)_2U[P(SiMe_3)_2](Cl)$ [14].

With **1** and **2**, a proton could not be transferred to the phosphido ligand to form the phosphine as in the case for the reaction with the primary bis(phosphido) complex, so the reaction with tBuNC was attempted, Equation (3). The ^{31}P NMR chemical shift for the thorium product, **3**, was observed at 58.5 ppm, while the $^{13}C\{^1H\}$ NMR spectrum showed a resonance at 265.4 ppm. These resonances are both shifted downfield from the other phosphazaaallene complexes, $(C_5Me_5)_2Th(C\equiv N^tBu)[\eta^2-N(^tBu)C=P(R)]$, R = Mes, Tipp, which have ^{31}P NMR resonances located at -10.7 ppm and -21.3 ppm, respectively. Further, the 1H NMR and ^{31}P NMR spectrum showed resonances for $P(SiMe_3)_2(C_6H_5)$ [37], the byproduct of silyl-extraction from one phosphido ligand. For **4**, a signal was located at 198.3 ppm in the ^{31}P NMR spectrum. Additionally, IR stretching frequencies at 2188 and 2171 cm^{-1} for **3** and **4**, respectively, were observed for the $C\equiv N$ bond of the tBuNC adduct.

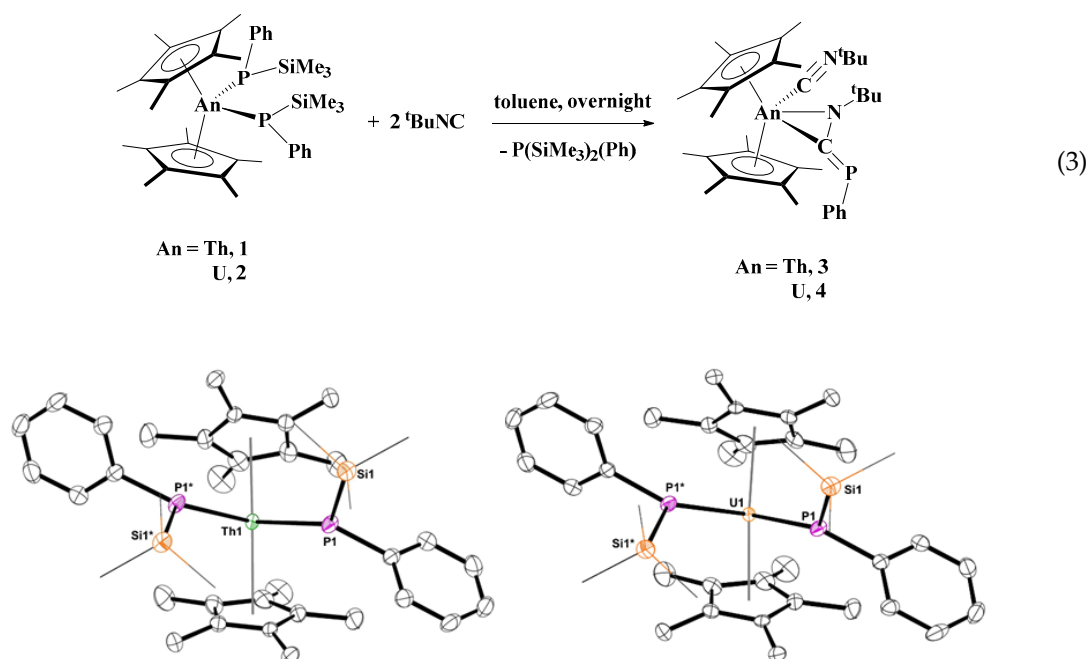


Figure 1. Thermal ellipsoid plots of **1** (left) and **2** (right) shown at the 50% probability level. Hydrogen atoms have been omitted and silyl groups shown in wireframe for clarity.

The structures of **3** and **4** were determined by X-ray crystallographic analysis and revealed the anticipated phosphazaallene complexes, Figure 2. Complex **4** is the first uranium complex with the phosphazaallene motif. The major difference between **3** and the previously reported structure, $(\text{C}_5\text{Me}_5)_2\text{Th}(\text{CN}^t\text{Bu})[\eta^2\text{-N}(^t\text{Bu})\text{C}=\text{P}(\text{Tipp})]$, Table 1, is the decrease in the steric properties of the phenyl versus 2,4,6- i -Pr₃C₆H₂ bound to phosphorus. As a result, the phenyl bends back towards the metal center in **3** with a Th–C26–P1 bond angle of 159.7(4)° and a C26–P–C(ipsos) bond angle of 102.3(4)°. These angles are 137.7(3)° and 115.8(3)°, respectively, in the tri(isopropyl)phenyl phosphazaallene complex. The actinide–nitrogen bond distance is 2.346(6) and 2.273(2) Å in **3** and **4**, respectively. The phosphazaallene moiety in **3** has a N2–C26 bond length of 1.367(9) Å and C26–P1 distance of 1.717(9) Å. There is a slight elongation of the C26–P1 bond in **4** to 1.733(3) Å with a subsequent and nearly equivalent contraction of the N2–C26 distance to 1.343(4) Å.

Due to the large bond dissociation energies for P–H and P–Si bonds of 297.0 kJ/mol and 363.3 kJ/mol [38], respectively, the formation of the phosphazaallene must be due to the kinetic lability of the phosphorus–element bond. Similar to the formation of the phosphazaallene previously reported [25], no detection of a phosphinidene intermediate was observed in the ³¹P NMR spectrum. This result, along with others, is consistent with insertion of the incoming substrate followed by bond activation without phosphinidene formation.

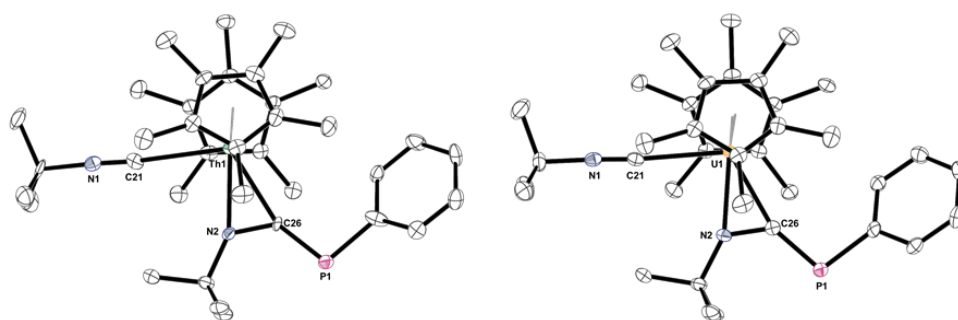


Figure 2. Thermal ellipsoid plots of **3** (left) and **4** (right) shown at the 50% probability level. Hydrogen atoms have been omitted for clarity.

Table 1. Selected bond distances (Å) and angles in **3** and **4** with comparison to the previously reported, $(C_5Me_5)_2Th(CN^tBu)[^tBuNC=PTipp]$, Tipp = 2,4,6- 1Pr_3C_6H_2 [25].

Bond Distance (Å)/Angle (deg)	3, An = Th	4, An = U	$(C_5Me_5)_2Th(CN^tBu)[N(^tBu)C=PTipp]$
An–N2	2.346(6)	2.273(2)	2.346(5)
An–C26	2.458(7)	2.383(3)	2.430(6)
N2–C26	1.367(9)	1.343(4)	1.348(8)
C26–P1	1.714(7)	1.733(3)	1.691(6)
An–C21	2.650(8)	2.568(3)	2.643(6)
N2–C26–P1	130.9(6)	130.4(2)	152.1(5)

3. Materials and Methods

General Considerations. All syntheses were carried out under inert atmosphere of nitrogen using standard Schlenk and glove box techniques. Solvents were purified in MBRAUN solvent purification system prior to use. *Tert*-butyl isocyanide (Aldrich, St. Louis, MO, USA) and $KN(SiMe_3)_2$ (Aldrich) were used as received. $(C_5Me_5)_2ThCl_2$ [39], and $(C_5Me_5)_2UCl_2$ [39], were prepared according to literature procedures. $KP[(C_6H_5)(SiMe_3)]$ was prepared from $HP[(C_6H_5)(SiMe_3)]$ and $KN(SiMe_3)_2$ in toluene and collected by filtration over medium porous frit followed by washing with toluene and drying under vacuum. Elemental analyses were performed at the University of California, Berkeley Microanalytical Facility using a Perkin–Elmer Series II 2400 CHNS analyzer (Waltham, MA, USA). C_6D_6 (Cambridge) was dried over molecular sieves and degassed with three cycles of freeze–pump–thaw. 1H and ^{13}C NMR experiment were performed on either Bruker Avance III 500 or 600 MHz spectrometer (Billerica, MA, USA). 1H and ^{13}C NMR spectrum are reported in ppm referenced internally to residual proton resonances. ^{31}P and ^{29}Si NMR experiment were performed on Bruker AVII+ 300 MHz spectrometer (Billerica, MA, USA). ^{31}P and ^{29}Si NMR are reported in ppm referenced external to 85% H_3PO_4 and $SiMe_4$, respectively. If coupling is not specified, then the origin is not definitively known. Infrared spectra were recorded as KBr pellets on Perkin–Elmer Spectrum One FT-IR spectrometer (Waltham, MA, USA).

Caution! Thorium-232 and depleted uranium (primarily U-238) are alpha-emitting radiometals with half-lives of 1.4×10^{10} years and 4.47×10^9 years, respectively. All work was carried out in a radiological laboratory with appropriate personal protective and counting equipment.

Synthesis of $(C_5Me_5)_2Th[P(C_6H_5)(SiMe_3)]_2$, 1. Toluene (10 mL) was added to a mixture of $(C_5Me_5)_2ThCl_2$ (200 mg, 0.35 mmol) and $KP(C_6H_5)(SiMe_3)$ (154 mg, 0.7 mmol). The resulting cloudy red solution was allowed to stir overnight, then filtered through a pipette plugged with Celite. Volatiles were removed in vacuo to yield an orange solid (253 mg, 84%). X-ray quality crystals of $(C_5Me_5)_2Th[P(C_6H_5)(SiMe_3)]_2$ were grown from a concentrated diethyl ether solution at $-45^\circ C$. 1H NMR (C_6D_6 , 600 MHz, 298 K): δ 7.74 (br-t, 4H, $J = 6.3$ Hz, *o*-Ph), 7.22 (t, 4H, $^3J_{H-H} = 7.2$ Hz, *m*-Ph), 7.12 (t, 2H, $^3J_{H-H} = 7.2$ Hz, *p*-Ph), 2.08 (s, 30H, C_5Me_5), 0.56 (d, 18H, $^2J_{H-P} = 4.2$ Hz, $SiMe_3$). $^{13}C\{^1H\}$ NMR (C_6D_6 , 150 Hz, 298 K): 140.4 (d, $^1J_{C-P} = 7.2$ Hz), 140.2 (t, $^2J_{C-P} = 3.15$ Hz), 128.1, 127.9, 126.6, 12.8, 3.7 (t, $J_{C-P} = 6$ Hz). $^{31}P\{^1H\}$ NMR (C_6D_6 , 120 MHz): δ 72.7. ^{29}Si INEPT NMR (C_6D_6 , 60 MHz): δ 5.62 (dd, $^1J_{Si-P} = 1.63$ Hz, $^1J_{Si-P} = 2.18$ Hz). IR (KBr, cm^{-1}): 2951 (m), 2898 (s), 2856 (m), 1576 (w), 1472 (w), 1431 (m), 1378 (w), 1247 (s), 1098 (s), 1024 (s), 897 (w), 835 (vs), 734 (m), 697 (m), 625 (w), 579 (w), 540 (w). Anal. Calcd for $C_{38}H_{58}P_2Si_2Th$: C, 52.76; H, 6.76. Found: C, 52.72; H, 6.65.

Synthesis of $(C_5Me_5)_2U[(P(C_6H_5)(SiMe_3)]_2$, 2. $(C_5Me_5)_2U[(P(C_6H_5)(SiMe_3)]_2$ was prepared in a manner similar to **1** except using $(C_5Me_5)_2UCl_2$ (126 mg, 0.22 mmol), $KP[(C_6H_5)(SiMe_3)]$ (144 mg, 0.65 mmol), and toluene (5 mL). The resulting deep brown solution was stirred overnight at room temperature, then, filtered through a pipette plugged with Celite. Volatiles were removed in vacuo to yield a dark brown solid. The residue was dissolved in pentane and filtered through Celite then isolated by concentration of the filtrate, causing crystallization of the product. The crystals were isolated and dried under vacuum (75 mg, 40%). 1H NMR (C_6D_6 , 600 MHz, 298 K): δ 13.5 (s, 30H,

C_5Me_5), -2.48 (s, 2H, Ph), -3.74 (s, 4H, Ph), -8.94 (s, 18H, SiMe₃), -28.6 (br-s, 4H, Ph). IR (KBr, cm⁻¹): 2955 (m), 2905 (br-s), 2859 (m), 1577 (w), 1474 (w), 1439 (br-m), 1378 (w), 1244 (m), 1137 (br-w), 1081 (w), 1064 (m), 1022 (m), 974 (w), 929 (br-w), 840 (vs), 750 (w), 727 (w), 695 (w), 630 (w). Anal. Calcd for C₃₈H₅₈P₂Si₂U: C, 52.40; H, 6.71. Found: C, 52.08; H, 6.52.

Synthesis of (C₅Me₅)₂U[(P(C₆H₅)(SiMe₃)](Cl), 2a. In a 20 mL scintillation vial, (C₅Me₅)₂UCl₂ (99 mg, 0.17 mmol), KP(C₆H₅)(SiMe₃) (38 mg, 0.17 mmol), and toluene (5 mL) were combined. The resulting deep brown solution was stirred overnight at room temperature and filter over a pipette plugged with Celite. Volatiles removed in vacuo to yield a deep brownish red solid (114 mg, 92%). ¹H NMR (C₆D₆, 600 MHz, 298 K): δ 13.4 (s, 30H, C₅Me₅), -5.59 (s, 2H, Ph), -5.96 (s, 1H, Ph), -13.9 (s, 9H, SiMe₃), -40.8 (s, 2H, Ph). IR (KBr, cm⁻¹): 2954 (m), 2905 (s), 2858 (m), 1579 (w), 1475 (m), 1438 (m), 1379 (m), 1259 (w), 1244 (m), 1144 (w), 1082 (s), 1066 (s), 1023 (s), 931 (m), 841 (vs), 800 (w), 751 (w), 727 (w), 694 (w), 631 (w). Anal. Calcd for C₂₉H₄₄Cl₁P₁Si₁U₁: C, 48.03; H, 6.12. Found: C, 48.45; H, 6.46.

Synthesis of (C₅Me₅)₂Th(C≡N^tBu)[(η²-N(^tBu)C=PPh)], 3. A solution of (C₅Me₅)₂Th[P(C₆H₅)(SiMe₃)]₂ (72 mg, 0.08 mmol) in methylcyclohexane (5 mL) was placed in a -45 °C freezer for 30 minutes prior to the next step. To this solution, an excess amount of *tert*-butyl isocyanide (0.15 mL, 1.3 mmol) was added dropwise. The mixture was allowed to stir at room temperature overnight, after which volatiles were removed in vacuo to yield an orange solid. An analytically pure sample of **3** was obtained after recrystallization in 1,2-dimethoxyethane (36 mg, 56%). X-ray quality crystals of **3** were grown from a concentrated 1,2-dimethoxyethane solution at -45 °C. ¹H NMR (C₆D₆, 600 MHz, 298 K): δ 8.22 (t, 2H, ³J_{C-H} = 6 Hz, *o*-Ph), 7.42 (t, 2H, ³J_{C-H} = 7.8 Hz, *m*-Ph), 7.19 (t, 1H, ³J_{C-H} = 7.2 Hz, *p*-Ph), 2.05 (s, 30H, C₅Me₅), 1.72 (d, 9H, *J* = 1.2 Hz, [(H₃C)₃C]NCPPh), 0.9 (s, 9H, (H₃C)₃CNC). ¹³C{¹H} NMR (C₆D₆, 150 MHz, 298 K): 265.4 (d, ¹J_{C-P} = 76.8 Hz), 155.7 (d, ¹J_{C-P} = 51.6 Hz), 131.5 (d, ³J_{C-P} = 18.6 Hz), 127.7 (d, ²J_{C-P} = 6.3 Hz), 123.8, 122.7, 61.6, 57.2, 29.7 (d, ⁴J_{C-P} = 12.8 Hz), 28.9, 12.0. ³¹P{¹H} NMR (C₆D₆, 120 MHz): δ 58.5. IR (KBr, cm⁻¹): 2966 (s), 2902 (s), 2860 (s), 2188 (vs), 1575 (m), 1470 (m), 1450 (m), 1436 (m), 1373 (m), 1355 (m), 1295 (vs), 1266 (s), 1235 (m), 1197 (s), 1086 (br-m), 1061 (m), 1023 (s), 936 (m), 838 (w), 825 (w), 802 (br-w), 749 (m), 736 (s), 698 (s), 638 (w), 590 (w), 546 (w), 525 (w). Anal. Calcd for C₃₆H₅₃N₂PTh: C, 55.66; H, 6.88; N, 3.61. Found: C, 55.42; H, 7.01; N, 3.54.

Synthesis of (C₅Me₅)₂U(C≡N^tBu)[(η²-N(^tBu)C=PPh)], 4. Complex **4** was prepared in a manner similar to **3** using (C₅Me₅)₂U[(P(C₆H₅)(SiMe₃)]₂ (241 mg, 0.28 mmol), *tert*-butyl isocyanide (0.1 mL, 0.88 mmol), and pentane (5 mL). The solution turned instantly from dark brown to black. An analytically pure sample of **4** was obtained after recrystallization in diethyl ether (87 mg, 40%). X-ray quality crystals of **4** were grown from a concentrated pentane solution at -45 °C. ¹H NMR (C₆D₆, 500 MHz, 298 K): δ 28.5 (s, 9H, ^tBu), 4.10 (s, 2H, Ph), 1.50 (s, 30H, C₅Me₅), -1.50 (s, 1H, Ph), -14.7 (s, 9H, ^tBu), -46.5 (s, 2H, Ph). ³¹P{¹H} NMR (C₆D₆, 120 MHz): δ 198.3. IR (KBr, cm⁻¹): 2967 (s), 2912 (s), 2171 (vs), 1438 (m), 1375 (m), 1262 (m), 1205 (br-m), 1082 (br-m), 1023 (m), 903 (w), 884 (w), 803 (br-m), 751 (w), 694 (w), 676 (w), 577 (w). Satisfactory elemental analysis could not be obtained after multiple attempts.

Crystallographic Data Collection and Structure Determination. The selected single crystals were mounted on Kapton cryoloops using viscous hydrocarbon oil. X-ray data collection was performed at 100(2) K. The X-ray data were collected on a Bruker D8 Venture diffractometer (Madison, WI, USA) equipped with a Photon 100 CMOS area detector using Mo-K α radiation from a microfocus source ($\lambda = 0.71073$ Å). The data collection and processing utilized Bruker Apex2 suite of programs [40]. The structures were solved using an iterative dual space approach as implemented in SHELXT [41] and refined by full-matrix least-squares methods on F2 using Bruker SHELX-2014/7 program. All non-hydrogen atoms were refined with anisotropic displacement parameters. All hydrogen atoms were placed at calculated positions and included in the refinement using a riding model. Thermal ellipsoid plots were prepared by using Olex2 [42] with 50% of probability displacements for non-hydrogen atoms. Crystal data and detail for data collection for complexes **1–4** are provided in Table 2, and Crystallographic Information Files (CIFs) are included in the Supplementary Materials.

Table 2. Crystallography parameters for complexes 1–4.

	1	2	3	4
CCDC deposit number	1826995	1826996	1826999	1827000
Empirical formula	C ₃₈ H ₅₈ P ₂ Si ₂ Th	C ₃₈ H ₅₈ P ₂ Si ₂ U	C ₃₆ H ₅₃ N ₂ PTh	C ₃₆ H ₅₃ N ₂ PU
Formula weight (g/mol)	865.00	870.99	776.81	782.80
Crystal habit, color	prism, red	plate, brown	prism, yellow	plate, brown
Temperature (K)	100(2)	100(2)	100(2)	100(2)
Space group	<i>P</i> 43 21 2	<i>P</i> 43 21 2	<i>P</i> 2 ₁ /c	<i>P</i> 2 ₁ /c
Crystal system	Tetragonal	Tetragonal	Monoclinic	Monoclinic
Volume (Å ³)	3988.1(9)	3927.8(8)	3516.2(6)	3469.4(2)
a (Å)	12.1642(12)	12.0767(11)	10.0829(10)	10.0337(4)
b (Å)	12.1642(12)	12.0767(11)	33.981(3)	33.6762(14)
c (Å)	26.953(3)	26.931(3)	10.7807(11)	10.7644(4)
α (°)	90	90	90	90
β (°)	90	90	107.8389(17)	107.477(1)
γ (°)	90	90	90	90
Z	4	4	4	4
Calculated density (mg/m ³)	1.441	1.473	1.467	1.499
Absorption coefficient (mm ⁻¹)	3.903	4.299	4.311	4.750
Final R indices [I > 2σ(I)]	R = 0.0203; wR2 = 0.0424	R = 0.0166; wR2 = 0.0330	R = 0.0594; wR2 = 0.1147	R = 0.0264; wR2 = 0.0459

Although the structure of **3** refined with satisfactory geometrical parameters, the model contained errors including anomalously large difference map holes, prolate/oblate thermal ellipsoids, and a high goodness of fit. Inspection of synthesized precession images from the diffraction photographs revealed the presence of at least one additional domain rotated slightly and largely overlapping with the first, suggesting a split crystal. The unit cell was re-determined with the program CELL_NOW using 1740 reflections with a signal-to-noise greater than 20 taken from 420 diffraction photographs. Of these, 1422 (82.1%) could be given *hkl* indices within ± 0.20 of integer values to a single domain. Including a second domain rotated by 1° with respect to the first increased this value to 1664 reflections (95.6%). Contribution from the additional crystallites was incorporated into the model using the SHELX TWIN command with the twin matrix output by CELL_NOW. The minor domain fraction refined to 9.43(3)%. Inclusion of the TWIN command improved but did not eliminate the problems with difference map and GooF, likely because there are additional unrefined domains.

4. Conclusions

In summary, the synthesis and characterization of two new actinide bis(phosphido) complexes and their reactivity with ^tBuNC has been investigated. Despite being secondary phosphido complexes, silyl migration from one phosphido to the other to form the parent phosphine and phosphazane moieties was observed in analogy to the reactivity observed previously with primary phosphido complexes.

Supplementary Materials: The following are available online at <http://www.mdpi.com/2304-6740/7/9/105/s1>: The CIFs and CheckCIFs.

Author Contributions: P.R., O.J.F., J.R.W. and S.P.K. worked together to conceive experimental design and write the manuscript. P.R. and O.J.F. executed the experimental work, while J.R.W. obtained funding. All authors contributed to writing of the manuscript.

Funding: We gratefully acknowledge support for this work from the U.S. Department of Energy, Office of Science, Early Career Research Program under Award DE-SC-0014174. We also thank the MU Honors College Discovery Fellows Program for partial support of O.J.F.

Conflicts of Interest: The authors declare no conflict of interest.

References

1. Bates, J.I.; Gates, D.P. Diphosphiranium (P_2C) or Diphosphetanium (P_2C_2) Cyclic Cations: Different Fates for the Electrophile-Initiated Cyclodimerization of a Phosphaalkene. *J. Am. Chem. Soc.* **2006**, *128*, 15998–15999. [[CrossRef](#)] [[PubMed](#)]
2. Martin, D.; Tham, F.S.; Baceiredo, A.; Bertrand, G. Synthesis of extended polyphosphacumulenes. *Chem. Eur. J.* **2006**, *12*, 8444–8450. [[CrossRef](#)] [[PubMed](#)]
3. Bates, J.I.; Kennepohl, P.; Gates, D.P. Abnormal reactivity of an N-heterocyclic carbene (NHC) with a phosphaalkene: A route to a 4-phosphino-substituted NHC. *Angew. Chem. Int. Ed.* **2009**, *48*, 9844–9847. [[CrossRef](#)] [[PubMed](#)]
4. Serin, S.C.; Pick, F.S.; Dake, G.R.; Gates, D.P. Copper(I) Complexes of Pyridine-Bridged Phosphaalkene-Oxazoline Pincer Ligands. *Inorg. Chem.* **2016**, *55*, 6670–6678. [[CrossRef](#)] [[PubMed](#)]
5. Dugal-Tessier, J.; Dake, G.R.; Gates, D.P. Chiral ligand design: A bidentate ligand incorporating an acyclic phosphaalkene. *Angew. Chem. Int. Ed.* **2008**, *47*, 8064–8067. [[CrossRef](#)] [[PubMed](#)]
6. Chen, L.; Rawe, B.W.; Adachi, K.; Gates, D.P. Phosphorus-Containing Block Copolymers from the Sequential Living Anionic Copolymerization of a Phosphaalkene with Methyl Methacrylate. *Chem. Eur. J.* **2018**, *24*, 18012–18019. [[CrossRef](#)] [[PubMed](#)]
7. Serin, S.C.; Dake, G.R.; Gates, D.P. Addition-Isomerization Polymerization of Chiral Phosphaalkenes: Observation of Styrene-Phosphaalkene Linkages in a Random Copolymer. *Macromolecules* **2016**, *49*, 4067–4075. [[CrossRef](#)]
8. Siu, P.W.; Serin, S.C.; Krummenacher, I.; Hey, T.W.; Gates, D.P. Isomerization Polymerization of the Phosphaalkene $MesP=CPh_2$: An Alternative Microstructure for Poly(methylenephosphine)s. *Angew. Chem. Int. Ed.* **2013**, *52*, 6967–6970. [[CrossRef](#)]
9. Rawe, B.W.; Gates, D.P. Poly(p-phenylenediethynylene phosphane): A Phosphorus-Containing Macromolecule that Displays Blue Fluorescence Upon Oxidation. *Angew. Chem. Int. Ed.* **2015**, *54*, 11438–11442. [[CrossRef](#)] [[PubMed](#)]
10. Dueck, K.; Rawe, B.W.; Scott, M.R.; Gates, D.P. Polymerization of 1-Phosphaisoprene: Synthesis and Characterization of a Chemically Functional Phosphorus Version of Natural Rubber. *Angew. Chem. Int. Ed.* **2017**, *56*, 9507–9511. [[CrossRef](#)] [[PubMed](#)]
11. Ritchey, J.M.; Zozulin, A.J.; Wroblewski, D.A.; Ryan, R.R.; Wasserman, H.J.; Moody, D.C.; Paine, R.T. An organothorium-nickel phosphido complex with a short thorium-nickel distance. The structure of $Th(\eta^5-C_5Me_5)_2(\mu-PPh_2)_2Ni(CO)_2$. *J. Am. Chem. Soc.* **1985**, *107*, 501–503. [[CrossRef](#)]
12. Hay, P.J.; Ryan, R.R.; Salazar, K.V.; Wroblewski, D.A.; Sattelberger, A.P. Synthesis and x-ray structure of $(C_5Me_5)_2Th(\mu-PPh_2)_2Pt(PMe_3)$: A complex with a thorium-platinum bond. *J. Am. Chem. Soc.* **1986**, *108*, 313–315. [[CrossRef](#)]
13. Wroblewski, D.A.; Ryan, R.R.; Wasserman, H.J.; Salazar, K.V.; Paine, R.T.; Moody, D.C. Synthesis and characterization of bis(diphenylphosphido)bis(pentamethylcyclopentadienyl)thorium(IV), $[(\eta^5-C_5(CH_3)_5)_2Th(PPh_2)_2]$. *Organometallics*. **1986**, *5*, 90–94. [[CrossRef](#)]
14. Hall, S.W.; Huffman, J.C.; Miller, M.M.; Avens, L.R.; Burns, C.J.; Sattelberger, A.P.; Arney, D.S.J.; England, A.F. Synthesis and characterization of bis(pentamethylcyclopentadienyl)uranium(IV) and -thorium(IV) compounds containing the bis(trimethylsilyl)phosphido ligand. *Organometallics* **1993**, *12*, 752–758. [[CrossRef](#)]
15. Edwards, P.G.; Harman, M.; Hursthouse, M.B.; Parry, J.S. The synthesis and crystal structure of the thorium tetraphosphido complex, $Th[P(CH_2CH_2PMe_2)_2]_4$, an actinide complex with only metal-phosphorus ligand bonds. *J. Chem. Soc. Chem. Commun.* **1992**, *19*, 1469–1470. [[CrossRef](#)]
16. Behrle, A.C.; Castro, L.; Maron, L.; Walensky, J.R. Formation of a Bridging Phosphinidene Thorium Complex. *J. Am. Chem. Soc.* **2015**, *137*, 14846–14849. [[CrossRef](#)] [[PubMed](#)]
17. Wildman, E.P.; Balazs, G.; Wooles, A.J.; Scheer, M.; Liddle, S.T. Thorium-phosphorus triamidoamine complexes containing Th–P single- and multiple-bond interactions. *Nat. Commun.* **2016**, *7*, 12884. [[CrossRef](#)]
18. Rookes, T.M.; Gardner, B.M.; Balazs, G.; Gregson, M.; Tuna, F.; Wooles, A.J.; Scheer, M.; Liddle, S.T. Crystalline Diuranium Phosphinidide and μ -Phosphido Complexes with Symmetric and Asymmetric UPU Cores. *Angew. Chem. Int. Ed.* **2017**, *56*, 10495–10500. [[CrossRef](#)] [[PubMed](#)]

19. Rookes, T.M.; Wildman, E.P.; Balazs, G.; Gardner, B.M.; Wooles, A.J.; Gregson, M.; Tuna, F.; Scheer, M.; Liddle, S.T. Actinide–Pnictide (An–Pn) Bonds Spanning Non-Metal, Metalloid, and Metal Combinations (An = U, Th; Pn = P, As, Sb, Bi). *Angew. Chem. Int. Ed.* **2018**, *57*, 1332–1336. [[CrossRef](#)] [[PubMed](#)]
20. Zhang, C.; Hou, G.; Zi, G.; Ding, W.; Walter, M.D. A Base-Free Terminal Actinide Phosphinidene Metallocene: Synthesis, Structure, Reactivity, and Computational Studies. *J. Am. Chem. Soc.* **2018**, *140*, 14511–14525. [[CrossRef](#)] [[PubMed](#)]
21. Zhang, C.; Hou, G.; Zi, G.; Ding, W.; Walter, M.D. An Alkali-Metal Halide-Bridged Actinide Phosphinidene Complex. *Inorg. Chem.* **2019**, *58*, 1571–1590. [[CrossRef](#)]
22. Zhang, C.; Hou, G.; Zi, G.; Walter, M.D. A base-free terminal thorium phosphinidene metallocene and its reactivity toward selected organic molecules. *Dalton Trans.* **2019**, *48*, 2377–2387. [[CrossRef](#)] [[PubMed](#)]
23. Zhang, C.; Wang, Y.; Hou, G.; Ding, W.; Zi, G.; Walter, M.D. Experimental and computational studies on a three-membered diphosphido thorium metallaheterocycle $[\eta^5\text{-}1,3\text{-(Me}_3\text{C)}_2\text{C}_5\text{H}_3]_2\text{Th}[\eta^2\text{-P}_2(2,4,6\text{-iPr}_3\text{C}_6\text{H}_2)_2]$. *Dalton Trans.* **2019**, *48*, 6921–6930. [[CrossRef](#)] [[PubMed](#)]
24. Edwards, P.G.; Hursthouse, M.B.; Abdul Malik, K.M.; Parry, J.S. Direct conversion of carbon monoxide to a coordinated secondary alcohol derivative by a thorium phosphido complex. *J. Chem. Soc. Chem. Commun.* **1994**, *10*, 1249–1250. [[CrossRef](#)]
25. Behrle, A.C.; Walensky, J.R. Insertion of ^tBuNC into thorium-phosphorus and thorium-arsenic bonds: Phosphaazaallene and arsaazaallene moieties in f element chemistry. *Dalton Trans.* **2016**, *45*, 10042–10049. [[CrossRef](#)] [[PubMed](#)]
26. Rungthanaphatsophon, P.; Barnes, C.L.; Kelley, S.P.; Walensky, J.R. Four-electron reduction chemistry using a uranium(III) phosphido complex. *Dalton Trans.* **2018**, *47*, 8189–8192. [[CrossRef](#)] [[PubMed](#)]
27. Vilanova, S.P.; Tarlton, M.L.; Barnes, C.L.; Walensky, J.R. Double insertion of benzophenone into thorium-phosphorus bonds. *J. Organomet. Chem.* **2018**, *857*, 159–163. [[CrossRef](#)]
28. Vilanova, S.P.; del Rosal, I.; Tarlton, M.L.; Maron, L.; Walensky, J.R. Functionalization of Carbon Monoxide and tert-Butyl Nitrile by Intramolecular Proton Transfer in a Bis(Phosphido) Thorium Complex. *Angew. Chem. Int. Ed.* **2018**, *57*, 16748–16753. [[CrossRef](#)] [[PubMed](#)]
29. Rungthanaphatsophon, P.; del Rosal, I.; Ward, R.J.; Vilanova, S.P.; Kelley, S.P.; Maron, L.; Walensky, J.R. Formation of an α -Diimine from Isocyanide Coupling Using Thorium(IV) and Uranium(IV) Phosphido-Methyl Complexes. *Organometallics* **2019**, *38*, 1733–1740. [[CrossRef](#)]
30. Garner, M.E.; Parker, B.F.; Hohloch, S.; Bergman, R.G.; Arnold, J. Thorium metallacycle facilitates catalytic alkyne hydrophosphination. *J. Am. Chem. Soc.* **2017**, *139*, 12935–12938. [[CrossRef](#)]
31. Rungthanaphatsophon, P.; Duignan, T.J.; Myers, A.J.; Vilanova, S.P.; Barnes, C.L.; Autschbach, J.; Batista, E.R.; Yang, P.; Walensky, J.R. Influence of Substituents on the Electronic Structure of Mono- and Bis(phosphido) Thorium(IV) Complexes. *Inorg. Chem.* **2018**, *57*, 7270–7278. [[CrossRef](#)] [[PubMed](#)]
32. Cendrowski-Guillaume, S.M.; Ephritikhine, M. Bispentamethylcyclopentadienyl uranium diphenylphosphide compounds. *J. Organomet. Chem.* **1999**, *577*, 161–166. [[CrossRef](#)]
33. Garner, M.E.; Arnold, J. Reductive elimination of diphosphine from a thorium-NHC-bis(phosphide) complex. *Organometallics* **2017**, *36*, 4511–4514. [[CrossRef](#)]
34. Frey, A.S.P.; Cloke, F.G.N.; Hitchcock, P.B.; Green, J.C. Activation of P₄ by U($\eta^5\text{-C}_5\text{Me}_5$)($\eta^8\text{-C}_8\text{H}_6(\text{Si}^i\text{Pr}_3)_2\text{-}1,4$) (THF); the x-ray structure of [U($\eta^5\text{-C}_5\text{Me}_5$)($\eta^8\text{-C}_8\text{H}_6(\text{Si}^i\text{Pr}_3)_2\text{-}1,4$)]₂($\mu\text{-}\eta^2\text{:}\eta^2\text{-P}_4$). *New J. Chem.* **2011**, *35*, 2022–2026. [[CrossRef](#)]
35. Patel, D.; Tuna, F.; McInnes, E.J.L.; Lewis, W.; Blake, A.J.; Liddle, S.T. An Actinide Zintl Cluster: A Tris(triamido-uranium) $\mu_3\text{-}\eta^2\text{:}\eta^2\text{:}\eta^2\text{-Heptaphosphanortricyclane}$ and Its Diverse Synthetic Utility. *Angew. Chem. Int. Ed.* **2013**, *52*, 13334–13337. [[CrossRef](#)] [[PubMed](#)]
36. Gardner, B.M.; Balazs, G.; Scheer, M.; Tuna, F.; McInnes, E.J.; McMaster, J.; Lewis, W.; Blake, A.J.; Liddle, S.T. Triamidoamine-Uranium(IV)-Stabilized Terminal Parent Phosphide and Phosphinidene Complexes. *Angew. Chem. Int. Ed.* **2014**, *53*, 4484–4488. [[CrossRef](#)] [[PubMed](#)]
37. Bailey, J.A.; Ploeger, M.; Pringle, P.G. Mono-, Di-, and Triborylphosphine Analogues of Triarylphosphines. *Inorg. Chem.* **2014**, *53*, 7763–7769. [[CrossRef](#)]
38. Luo, Y.R. *Comprehensive Handbook of Chemical Bond Energies*; CRC Press: Boca Raton, FL, USA, 2007.
39. Fagan, P.J.; Manriquez, J.M.; Maatta, E.A.; Seyam, A.M.; Marks, T.J. Synthesis and properties of bis(pentamethylcyclopentadienyl) actinide hydrocarbyls and hydrides. A new class of highly reactive f-element organometallic compounds. *J. Am. Chem. Soc.* **1981**, *103*, 6650–6667. [[CrossRef](#)]

40. Bruker AXS Inc. *APEX2 Suite*; Bruker AXS Inc.: Madison, WI, USA, 2006.
41. Sheldrick, G.M. *SHELXT*—Integrated space-group and crystal-structure determination. *Acta Cryst. Sect. A Found. Adv.* **2015**, *71*, 3–8. [[CrossRef](#)]
42. Dolomanov, O.V.; Bourhis, L.J.; Gildea, R.J.; Howard, J.A.K.; Puschmann, H. *OLEX2*: A complete structure solution, refinement and analysis program. *J. Appl. Cryst.* **2009**, *42*, 339–341. [[CrossRef](#)]



© 2019 by the authors. Licensee MDPI, Basel, Switzerland. This article is an open access article distributed under the terms and conditions of the Creative Commons Attribution (CC BY) license (<http://creativecommons.org/licenses/by/4.0/>).